ISBN: 978-3-95450-231-8 ISSN: 2673-5490 doi: 10.18429/JACoW-IPAC2023-TUPA160

VALIDATION OF CONTROL LOOP MODELING FOR POWER LIMITATION STUDIES WITH BEAMS FOR HL-LHC

B. E. Karlsen-Bæck*[1], T. Argyropoulos, R. Calaga, I. Karpov, H. Timko
CERN, Meyrin, Switzerland
[1]also at the Department of Physics, Sapienza Università di Roma, Rome, Italy

Abstract

For HL-LHC intensities, transient beam loading after injection between the Super Proton Synchrotron (SPS) and the Large Hadron Collider (LHC) is expected to push the RF power in the LHC to the limit of the installed system. A detailed understanding of this process is necessary to minimize beam losses during LHC injection. Realistic models of the local SPS and LHC cavity control systems were implemented in the Beam Longitudinal Dynamics (BLonD) simulation suite to model bucket-by-bucket and turn-by-turn transient effects. We show the results of studies and detailed benchmarks of key observables such as bunch-by-bunch spacing, RF power at 2023 beam intensity and transfer functions against theory and measurements.

INTRODUCTION

For a bunch intensity target of 2.3×10^{11} protons per bunch (p/b) for HL-LHC [1], it is expected that the minimum average klystron forward power in steady state is close to 265 kW [2, 3]. This assumes the half-detuning beam-loading compensation scheme [4] to optimize the average power required during the injection process. The design power of an LHC klystron is 300 kW [5], with one klystron per cavity, and eight cavities being installed per beam. Line-by-line measurements of the klystron power at saturation range between 280 kW and 310 kW. An operational margin is typically required for regulating feedback loops and remain below the saturation region. Furthermore, at injection, steady state conditions are not satisfied. During the bunch-to-bucket transfer from the SPS to the LHC, there are both bucket-by-bucket transients due to feedback loops and turn-by-turn transients due to the unmatched beam. Taking all the above into account, at HL-LHC intensities, the capture voltage should be minimized while keeping beam losses small [6, 7], as well as a mitigation of longitudinal instabilities at injection [8, 9]. Simulations are best suited to predict the injection dynamics, and with it the demanded RF power, for HL-LHC.

To accurately predict the longitudinal beam behavior after injection into the LHC, realistic models of the cavity loops are needed. The models are implemented in the simulation suite Beam Longitudinal Dynamics (BLonD) [10] and benchmarked against both theory and measurements, with and without beam.

* birk.beck@cern.ch

THE SPS AND LHC CAVITY CONTROLLER MODELS

The cavity controller models in both the SPS and the LHC determine the RF beam current from the line density of the projected particle distribution in BLonD and apply a correction to the RF voltage that acts on the beam. With respect to the RF voltage V_{rf} and phase ϕ_{rf}, the effective voltage including feedbacks becomes

$$V_{\mathrm{eff}}(\Delta t) = \frac{|V_{\mathrm{ant}}|}{|V_{\mathrm{set}}|}\,|V_{\mathrm{rf}}|\,\sin\left(\omega_{\mathrm{rf}}\Delta t + \phi_{\mathrm{rf}} + \phi_{\mathrm{ant}} - \phi_{\mathrm{set}}\right), \quad (1)$$

where ω_{rf} is the angular RF frequency, Δt is the longitudinal time coordinate, while $|V_{\mathrm{set}}|$ and ϕ_{set} is the set point voltage amplitude and phase, respectively. $|V_{\mathrm{ant}}|$ and ϕ_{ant} are the gap voltage amplitude and phase and is given by

$$V_{\mathrm{ant}} = V_{\mathrm{gen}} + V_{\mathrm{beam}}\,, \quad (2)$$

where V_{gen} and V_{beam} are the generator-induced and beam-induced voltages in the cavity, respectively. In the BLonD model these signals are resolved both on a coarse sample grid, representing the sampling in the real system, and a fine grid, used to interface with the particle tracking. The resolution of the coarse grid is $N_{\mathrm{res}}T_{\mathrm{rf}}$ and the fine grid has the same resolution as the binning of the beam line density. N_{res} is 5 in the SPS cavity controller model and 10 in the LHC model, which corresponds to one sample per bunch in each machine.

The SPS One-Turn Delay Feedback Model

In the SPS, the one-turn delay feedback (OTFB) is used to regulate the gap voltage V_{ant} in each traveling wave cavity (TWC) to match the set point voltage V_{set}. Both the generator-induced and the beam-induced voltages are computed in time domain through a matrix convolution [11]

$$\begin{bmatrix} V_I(t) \\ V_Q(t) \end{bmatrix} = H * \vec{I} = \begin{bmatrix} h_s(t) & -h_c(t) \\ h_c(t) & h_s(t) \end{bmatrix} * \begin{bmatrix} I_I(t) \\ I_Q(t) \end{bmatrix}, \quad (3)$$

where the H is the response matrix. The elements of the generator response matrix and the beam response matrix are found from the TWC impedance towards the generator and towards the beam, respectively [11].

The LHC Cavity Loop Model

In the LHC, both a direct RF feedback (RFFB) and a OTFB are applied to regulate the RF voltage [12]. Using the relationship between the generator current I_{gen}, gap voltage and RF beam current $I_{\mathrm{beam,rf}}$ in [13], it is possible to show

ISBN: 978-3-95450-231-8 ISSN: 2673-5490 doi: 10.18429/JACoW-IPAC2023-TUPA160

that in the LHC cavity model, the gap voltage is given as an iterative sample-by-sample equation;

$$V_{\text{ant}}^{(n)} = \left(1 - \frac{\omega_{\text{rf}} T_s}{2Q_L} + i\Delta\omega T_s\right) V_{\text{ant}}^{(n-1)} + (R/Q)\,\omega_{\text{rf}} T_s \left(I_{\text{gen}}^{(n-1)} - \frac{1}{2} I_{\text{beam,rf}}^{(n-1)}\right). \quad (4)$$

Here, Q_L is the loaded quality factor, T_s is the sampling time, $\Delta\omega = \omega_r - \omega_{\text{rf}}$ is the detuning of the RF cavity and (R/Q) is the cavity R upon Q. Additionally, ω_r is the angular resonance frequency of the RF cavity. The superscript n in the signals denotes the sample number. In the model, this equation is solved both on the coarse and fine grid. The coarse-grid gap voltage is then used to compute an error signal, which is injected into the LHC OTFB and the RFFB signal processing. The RFFB model consists of an analog branch acting as a high-pass filter and a digital branch acting as a low-pass filter [12]. The OTFB sits on the analog branch to boost analog gain and counteract coupled-bunch instabilities.

BENCHMARKING THE SPS MODEL

Both models were first benchmarked without beam. This was done by simulating base-band network analyzer measurements of the models under different configurations. Validation was done for the SPS OTFB against the theoretically expected response. Additionally, the Nyquist plot of the simulated transfer function shows that the model gives the expected linear total gain, overall phase and the correct stability margin [14].

For the SPS machine, with a bunch in every fifth RF bucket, the signals in the SPS OTFB reach steady state. For this theoretical case, it is possible to compute these steady-state values of the power and RF voltage analytically and hence verify that the model gives correct estimates [14]. The SPS 200 MHz RF system consists of four 3-section and two 4-section TWCs and the total RF voltage is partitioned between the two types [15]. Table 1 shows results from simulation and the theoretical values. The SPS OTFB model seems to agree well with theory when assuming a finite factor of 20 linear (26 dB) total gain of the loop.

Table 1: Transmitter forward power of the SPS 3-section TWC at flattop. A bunch length of 1.2 ns and a bunch intensity of 2.3×10^{11} p/b was assumed, giving an RF peak beam current of $I_b = 2.75$ A. The total voltage was 10 MV and 51.7 % of it was distributed to the 3-section cavities.

Config.	Theory	Sim.
No beam	442.8 kW	430.1 kW
Beam	717.9 kW	711.1 kW

In BLonD it is possible to generate beams that are well matched to a given potential with correct bunch length and intensity, but the dynamics of the SPS OTFB model is needed to recreate the correct bunch-by-bunch spacing. The SPS OTFB model was benchmarked against measurements of the "standard" 25 ns LHC type beam in the SPS consisting of four 72 bunch batches at flattop (440 GeV) to verify that it could reproduce the bunch-by-bunch spacing. Longitudinal beam profile measurements were taken from a wall-current monitor, analyzed and reconstructed in simulations. The simulations were then run with the parameters of the measured cycle and the beam recreated from the measured bunch lengths τ_b and bunch intensities N_b. Figure 1 illustrates the agreement between the simulated and measured bunch-by-bunch position variation of the first batch. The TWC central frequencies ω_c used in these simulations are found in [14]. There were uncertainties in the gain of the OTFB, the real RF voltage in the measured cycle and ω_c of the TWCs, which could explain the difference between measurements and simulations near the start and end of the batch. The overall agreement is excellent when considering these sources of error.

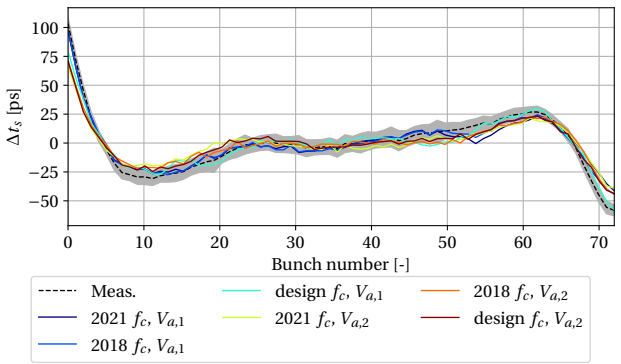

Figure 1: Measured and simulated bunch-by-bunch position variation for different TWC central frequencies and different total gap voltages ($V_{a,1} = 5.89$ MV and $V_{a,2} = 6.76$ MV).

BENCHMARKING THE LHC MODEL

As a first test of the LHC cavity loop model, the transfer function of the system was simulated in both closed-loop and open-loop configurations and compared with measurements taken during commissioning. Both settings show good agreement with measurements [14].

Comparisons with data at LHC flat-bottom after multiple injections were used to benchmark the LHC cavity loop model with beam in steady-state conditions. The simulation was done at LHC flat-bottom (450 GeV) with 1992 bunches, 1.4×10^{11} p/b, a bunch length of 1.25 ns, $Q_L = 2 \times 10^4$, a $\Delta\omega$ of -13.135 kHz and 4 MV total RF voltage. In simulations, the beam model was simplified to a rigid beam of identical bunches due to the large amount of macroparticles needed otherwise. Figure 2 shows the amplitude and phase of the RF power computed by the model. The agreement is good for the no-beam segment (65 μs to 90 μs) and the later injected batches from around 40 μs onwards in Fig. 2. However, for the initially injected batches, at around 0 to 20 μs, there is a difference between simulation and measure-

ISBN: 978-3-95450-231-8 ISSN: 2673-5490 doi: 10.18429/JACoW-IPAC2023-TUPA160

ment. This is likely due to the beam phase loop causing a spread, both bunch-by-bunch and batch-by-batch, in intensity, bunch length and bunch spacing, which in general will lead to a difference in transients for different batches. In addition, there is a 20 % uncertainty in the measurement of the generator forward power in Fig. 2. Considering this, the agreement is good and the benchmark illustrates that the model can reproduce bucket-by-bucket power transients which will be essential for injection studies for HL-LHC.

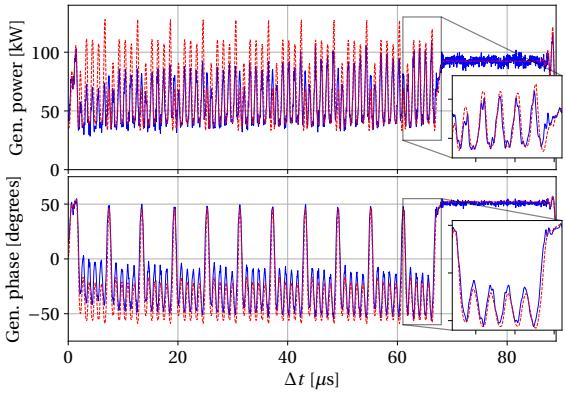

Figure 2: Power amplitude and phase from measurements of cavity 8B1 (blue) and simulations (red) at 450 GeV with 1992 bunches.

Lastly, the LHC cavity loop was benchmarked against measured data at injection, using high-intensity beams at about 1.8×10^{11} p/b to verify turn-by-turn power transients when steady-state is not yet reached. A 36 bunch SPS batch was recreated at SPS flattop based on measurements to obtain the correct spread in bunch length and intensity, and simulated for 10 000 turns with the SPS OTFB model to obtain the correct bunch spacing. The batch was then simulated in the LHC using the cavity loop. Figure 3 depicts the bunch-by-bunch position variation of the beam in the simulation at turn zero in the LHC, which also illustrates that the SPS OTFB model can reproduce the bunch-by-bunch phase offset of shorter batches. In reality a 12 bunch batch was already circulating in the LHC. The 12 bunch batch was recreated in the same way as the ones with 36 bunches and simulated for 200 turns before the 36 bunch injection to more accurately reproduce the transients.

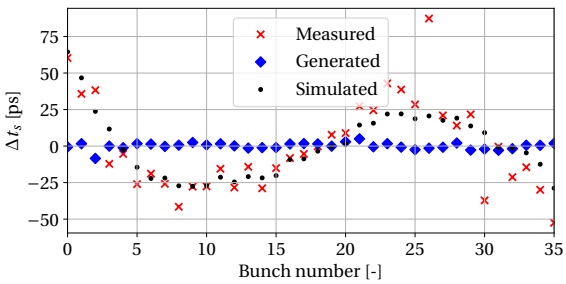

Figure 3: Bunch-by-bunch position variation of a 36 bunch beam in the SPS from measurement, generation without SPS OTFB and tracking with the SPS OTFB.

Approximately 25 turns of data was taken after injection during the measurement. The measured and simulated peak turn-by-turn value of the generator forward power is found in Fig. 4. The shaded areas represent the variation in peak power from the eight cavities in the two LHC rings, B1 and B2. The 36 bunch batch injected into the two rings had different intensities, which is why a systematic difference in the maximum power between both is observed. The simulated beam was generated using the parameters of beam 1 at injection. The simulation parameters of the cavity loop was chosen such that it would match a cavity with a representative no beam segment with low signal noise. Measurements from some of the cavities were noisy and therefore had a higher peak power, which is why it is expected that the simulated transient is in the lower part of the shaded area. The simulated model matches the measurement very well and the difference seen at turn 2 in Fig. 4 is likely due to fine-tuning of the parameters in the model.

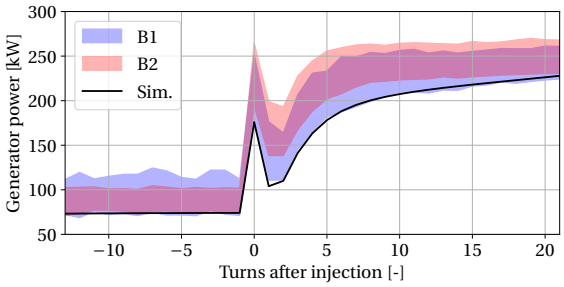

Figure 4: The peak power for each turn upon injection of a 36 bunch batch from measurements of ring 1 (B1), ring 2 (B2) and simulation (Sim.). The shaded areas were obtained from the spread of the turn-by-turn peak power among the eight RF systems.

CONCLUSION

Models of both the SPS and the LHC cavity loops have been implemented in BLonD and benchmarked in detail. Transfer function simulations of both models give good agreement with measurements. Furthermore, the SPS model recreates the bunch-by-bunch parameters of the beam at flattop well, which will be essential for loss studies at LHC injection for future high-intensity operation. Lastly, the LHC model is able to accurately recreate transients in generator power both in steady-state and at bunch-to-bucket transfer. The next step will be to benchmark the SPS feed-forward, couple the local and global feedbacks and apply them to study RF power limitations and beam losses for HL-LHC.

ACKNOWLEDGEMENTS

Research supported by the HL-LHC project. We would like to thank P. Baudrenghien, D. Quartullo, A. Lasheen, H. Damerau and M. Zampetakis for useful comments and discussions. Additionaly, we would like to thank A. Butterworth, D. A. Długosz and the SPS and LHC shift crews for help with measurements.

ISBN: 978-3-95450-231-8 ISSN: 2673-5490 doi: 10.18429/JACoW-IPAC2023-TUPA160

REFERENCES

[1] O. Aberle *et al*. "High-Luminosity Large Hadron Collider (HL-LHC): Technical design report", CERN Yellow Reports: Monographs, Rep. CERN-2020-010, CERN, Geneva, Switzerland, 2020

[2] O. Brüning *et al*. "LHC Design Report", CERN Yellow Reports: Monographs, Rep. CERN-2004-003-V-1, CERN, Geneva, Switzerland, 2004

[3] H. Timko, Talk at Chamonix 2022, https://indico.cern.ch/event/1097716/contributions/4618900/

[4] D. Boussard, "rf power requirements for a high intensity proton collider ; parts 1 (chapters I, II, III) and 2 (chapters IV, V, VI)", Rep. CERN-SL-91-16-RFS, CERN, Geneva, Switzerland, 1991.

[5] O. Brunner *et al*., "RF Power Generation in LHC", *in Proc. of IEEE Particle Accelerator Conference 2003*, Portland, OR, USA, 2003.

[6] L. Medina *et al*., "Optimal injection voltage in the LHC", *Nucl. Instrum. Methods Phys. Res., A*, vol. 1039, p. 166994, 2022, doi:10.1016/j.nima.2022.166994

[7] L. Medina *et al*., "Studies of Longitudinal Beam Losses at LHC Injection", *in Proc. of International Particle Accelerator Conference 2021*, p. 4164-416, 2021, doi:10.18429/JACoW-IPAC2021-THPAB199

[8] H. Timko *et al*., "Beam Instabilities after Injection to the LHC", *in Proc. of ICFA ABDW on High-Intensity and High-Brightness Hadron Beams 2018*, p. TUP1WA03, Daejeon, Korea, 2018, doi:10.18429/JACoW-HB2018-TUP1WA03

[9] I. Karpov *et al*., "Consequences of longitudinal coupled-bunch instability mitigation on power requirements during the HL-LHC filling", *in Proc. of ICFA mini-Workshop on Mitigation of Coherent Beam Instabilities in Particle Accelerators 2019*, Zermatt, Switzerland, 2019, *doi:10.23732/CYRCP-2020-009.312*

[10] H. Timko *et al*., "Beam Longitudinal Dynamics Simulation Suite BLonD", 2022, arXiv:2206.08148.

[11] P. Baudrenghien and T. Mastoridis, "I/Q Model of the SPS 200 MHz Travelling Wave Cavity and Feedforward Design", Rep. CERN-ACC-NOTE-2020-0032, CERN, Geneva, Switzerland, May 2020.

[12] P. Baudrenghien *et al*., "The LHC Low Level RF", Rep. CERN-LHC-PROJECT-Report-906, CERN, Geneva, Switzerland, 2006.

[13] J. Tückmantel, "Cavity-beam-transmitter interaction formula collection with derivation", Rep. CERN-ATS-Note-2011-002-TECH, CERN, Geneva, Switzerland, Jan. 2011.

[14] B. E. Karlsen-Bæck, "Modelling Control Loops for SPS-LHC Beam Transfer Studies", MSc Thesis, Norwegian University of Science and Technology (NTNU), Norway, Rep. CERN-THESIS-2022-159, CERN Geneva, Switzerland, 2022, https://cds.cern.ch/record/2837220

[15] G. Dôme, "The SPS acceleration system travelling wave drift-tube structure for the CERN SPS", *in Proc. of Linear Accelerator Conference 1976*, Chalk River, Canada, 1976.